Journal of Molecular Catalysis A: Chemical 350 (2011) 69–74

Contents lists available at SciVerse ScienceDirect

Journal of Molecular Catalysis A: Chemical

journal homepage: www.elsevier.com/locate/molcata

# Effect of interaction between Ni and YSZ on coke deposition during steam reforming of methane on Ni/YSZ anode catalysts for an IR-SOFC

Hiroki Takahashi[a], Tatsuya Takeguchi[a,*], Norikazu Yamamoto[a], Motofumi Matsuda[b], Eiko Kobayashi[a], Wataru Ueda[a]

[a] Catalysis Research Center, Hokkaido University, Kita 21 Nishi 10, Kita-ku, Sapporo 001-0021, Japan
[b] Santoku corporation, 4-14-34, Fukae-kitamachi, Higashinada-ku, Kobe 658-0013, Japan

ARTICLE INFO

*Article history:*
Received 3 June 2011
Received in revised form
12 September 2011
Accepted 12 September 2011
Available online 18 September 2011

*Keywords:*
Ni cermet
Support crystallite size
Interaction
Surface hydroxide group

ABSTRACT

Ni cermet anodes were prepared from nanoparticle 8 mol% yttria-stabilized zirconia (8YSZ) with various crystallite sizes. Results of temperature-programmed reduction of the anode suggested strong interaction between Ni and 8YSZ with a small crystallite size. The performance of an internal reforming solid oxide fuel cell (IR-SOFC) with anodes prepared from 8YSZ was almost the same regardless of interaction between Ni and 8YSZ. However, the rate of coke deposition decreased with an increase in interaction between Ni and 8YSZ. This strong interaction was caused by the presence of surface hydroxide groups indicated by in situ FT-IR. Carbon deposition resistance was enhanced by controlling the interaction between Ni and 8YSZ.



## 1. Introduction

Power generation by solid oxide fuel cells (SOFCs) is one of the most attractive energy conversion systems because of their high efficiency, low pollution and fuel flexibility. The high operation temperature allows an SOFC to operate on a large range of fuels, including hydrocarbon [1–3], coal syngas [4,5], biogas [6], and even solid carbon [7]. Among these fuels, natural gas has attracted great interest because it is a relatively cheap and widely available fuel with many deposits; thus, it is suitable for SOFCs. The composition of natural gas, depending on the place of production, is basically methane with a small amount of other hydrocarbons and a tiny amount of impurities. Methane can be reformed into $H_2$ as follows. Steam reforming of methane:

$$CH_4 + H_2O \rightarrow 3H_2 + CO \quad (1)$$

Water gas shift reaction:

$$CO + H_2O \rightarrow CO_2 + H_2 \quad (2)$$

Nickel/yttria-stabilized zirconia (Ni/YSZ) cermet is most commonly used as an IR-SOFC anode catalyst due to its high activity for electrochemical fuel oxidation reaction and compatibility of thermal expansion coefficient to electrolytes such as YSZ. Even thermodynamically carbon deposition-free condition (TCDC), carbon is kinetically deposited on a Ni/YSZ anode catalyst during internal reforming of methane (Eq. (1)). Eq. (1) is consisted of Eqs. (3) and (4).

A considerably larger amount of water is added to a reactor because the rate of methane cracking (Eq. (3)) is high on a Ni catalyst.

$$CH_4 \rightarrow C + 2H_2 \quad (3)$$

$$C + H_2O \rightarrow CO + H_2 \quad (4)$$

Carbon deposition for an IR-SOFC causes deactivation of the Ni catalyst and rapid degradation of IR-SOFC performance. Thus, it is important to achieve the catalytic reforming activity and tolerance to carbon deposition. Some efforts have been made to suppress carbon deposition. The addition of alkaline earth oxide (MgO, CaO, and SrO) and $CeO_2$ to Ni/YSZ cermet has been reported [8]. Although addition of CaO addition is effective for suppressing carbon deposition and promoting reforming, electrochemical activity as anode is slightly reduced. Matsui et al. reported that the carbon deposition over cermets proceeded readily when the source oxide mixuture (NiO/Scandia-stabilized zirconia, NiO/ScSZ) was treated at high temperature as compared to that treated at low temperature. This can be explained by strong interaction between NiO and ScSZ as well as the agglomeration of Ni particles [3]. Carbon formation in the presence of hydrocarbons can be avoided by replacing Ni

* Corresponding author. Tel.: +81 11 706 9165; fax: +81 11 706 9163.
*E-mail address:* takeguch@cat.hokudai.ac.jp (T. Takeguchi).

1381-1169/$ – see front matter © 2011 Elsevier B.V. All rights reserved.
doi:10.1016/j.molcata.2011.09.007

with a metal that does not catalyze C–C bond formation, such as Cu, but the thermal stability of alternative electrodes tends to be worse [9–11]. Oxide anodes (especially perovskite-type oxide) have been reported as alternative SOFC anodes because oxides are not expected to catalyze the formation of carbon [12–14]. However, it is difficult to apply an oxide anode for an SOFC because the catalytic performance for steam reforming and electro oxidation of $H_2$ is insufficient. Therefore, the carbon deposition resistance of Ni/YSZ should be improved. The effect of preheat-treatment of YSZ prepared by the glycothermal method before mixing Ni and YSZ was therefore investigated.

## 2. Experimental methods

Nanoparticle 8YSZ powders having a large surface area were prepared by the glycothermal method [15]. One bottle of 70% $Zr(OC_3H_7)_4$ in 1-propanol (25 g, Kishida Chemical Co., Ltd) and 3.14 g of $(CH_3COO)_3Y{\cdot}4H_2O$ (Wako Pure Chemical Industries, Ltd) were mixed in 100 ml of 1,4-butanediol (Wako Pure Chemical Industries, Ltd) in a test tube, which was then set in a 300 ml autoclave. An additional 30 ml of 1,4-butanediol was added to the gap between the test tube and autoclave. The gas phase in the autoclave was replaced with Ar gas. The mixture was heated from room temperature to 300 °C at a rate of 2.3 °C $min^{-1}$ and kept at that temperature for 2 h. After cooling, the resulting powders were washed with ethanol and dried at room temperature for one day. The dried powders were calcined at various temperature with a heating rate of 3.3 °C $min^{-1}$, giving three kinds of 8YSZ, which were then calcined at 600 °C or 1000 °C or not calcined; they were denoted as 8YSZ-600, 8YSZ-1000 and 8YSZ-non, respectively. They were impregnated with $Ni(NO_3)_2{\cdot}6H_2O$ (Wako Pure Chemical Industries, Ltd) aqueous solution with an Ni loading of 44 wt%. Generally, high Ni loading have been used for SOFC anode [16–18]. The impregnated powders were calcined at 1400 °C at a rate of 3.3 °C $min^{-1}$ and kept at that temperature for 4 h to form Ni/8YSZ, and they were denoted as Ni/8YSZ-600-1400, Ni/8YSZ-1000-1400 and Ni/8YSZ-non-1400, respectively.

One side of a YSZ disk (20 mm in diameter, 0.5 mm in thickness) was painted with the slurry of a mixture of polyethylene glycol 600 and the above-mentioned cermet. The painted disk was heated from room temperature to 1400 °C at a rate of 3.3 °C $min^{-1}$ and kept at that temperature for 4 h in air.

A perovskite-type $La_{0.6}Sr_{0.4}MnO_3$ mixed oxide was also prepared for the cathode catalyst. Desired amounts of $(CH_3COO)_3La{\cdot}nH_2O$, $(CH_3COO)_2Sr{\cdot}(1/2)H_2O$, and $(CH_3COO)_2Mn{\cdot}4H_2O$ (Wako Pure Chemical Industries, Ltd.) were dissolved in distilled water. The water was removed from the mixed solution at 100 °C and the powders were dried at 120 °C overnight. The dried powders were ground in a motor-driven mill for 24 h. The ground powders were heated from room temperature to 900 °C at a rate of 3.3 °C $min^{-1}$ and kept at that temperature for 10 h to form perovskite-type $La_{0.6}Sr_{0.4}MnO_3$ oxide. The slurry of a mixture of polyethylene glycol 600 and $La_{0.6}Sr_{0.4}MnO_3$ was applied on the other side of the disk. The disk with both sides painted was heated from room temperature to 1150 °C at a rate of 3.3 °C $min^{-1}$ and kept at that temperature for 5 h in air. The area of the electrode was 0.28 $cm^2$.

Crystal structure and crystallite size were determined using XRD measurements. XRD powder patterns were obtained on a Rigaku RINT-Ultima+ X-ray diffractometer using a Cu Kα X-ray source (40 kV, 20 mA). All samples were scanned at a 2$\theta$ range of 20–80° at a scanning rate of 2.000°/min.

The rate of coke deposition was measured on a Shimadzu TGA 50 micro-thermobalance. Catalyst sample was filled in platinum pan, which was set in apparatus. First, 5% $H_2$–Ar was fed to the sample at a flow rate of 60 STP ml $min^{-1}$ during programmed heating to 1000 °C at 10 K $min^{-1}$ to reduce NiO. When the temperature reached to 1000 °C, 5% $H_2$–Ar was switched to mixed gas composed of 19.3% $CH_4$, 10.6% $H_2O$ and balance $N_2$ was fed at 1000 °C and at a flow rate of 60 STP ml $min^{-1}$. The catalyst weight was varied depending on the catalytic activity to fix methane conversion to 35%. The rate of coke deposition was determined by measuring the amount of carbon deposited for the first 10 min.

Temperature-programmed reduction (TPR) was conducted using CHEMBET-3000 (Yuasa Ionics Inc.). The catalyst sample was reduced in 5% $H_2$–Ar at a flow rate of 70 ml $min^{-1}$ (25 °C, 1 atm) with a heating rate of 10 K $min^{-1}$. In situ DRIFTS measurements were carried by using a JASCO FT/IR-6100 spectrometer equipped with MCT detector. IR spectra were measured from 100 °C to 400 °C under He flow.

The current–voltage characteristics were measured at a cell temperature of 1000 °C on Autolab30-MF-SP by using General Purpose Electrochemical System for Windows version 4.9 (Autolab Eco Chemie B.V.). Before measurement, pure $H_2$ was fed to anode to reduce NiO at 1000 °C. After reduction of NiO, a gas mixture of 97% $H_2$ and 3% $H_2O$ was supplied as anode gas to Ni/8YSZ and $O_2$ was fed to the $La_{0.6}Sr_{0.4}MnO_3$ cathode at a flow rate of 100 STP ml $min^{-1}$. For IR-SOFC measurement, a gas mixture of 10% $CH_4$, 20% $H_2O$ and 70% $N_2$ was supplied as anode gas to Ni/8YSZ. The AC impedances were measured at a cell temperature of 1000 °C on Autolab30-MF-SP by using Frequency Response Analyser Windows version 4.9 (Autolab Eco Chemie B.V.) at open circuit voltage in the frequency range from 0.1 Hz to 10 kHz with signal amplitude of 10 mV.

## 3. Results and discussion

### 3.1. Structural analysis (XRD)

Fig. 1 shows XRD patterns for 8YSZ-non, 8YSZ-600 and 8YSZ-1000. The peaks of 8YSZ-non and 8YSZ-600 were broad, indicating that the formed powders were composed of fine crystallites. The crystallite sizes of 8YSZ-non, 8YSZ-600 and 8YSZ-1000 were 3, 5 and 20 nm, respectively. The XRD patterns indicated that the formed powders were composed of mixed oxides having tetragonal or cubic structures. The peak width for the mixed oxides for 8YSZ-non and 8YSZ-600 was too large to distinguish tetragonal and cubic structures. The peaks of 8YSZ-1000 were much sharper than those of 8YSZ-non and 8YSZ-600, indicating that fine particles grew to large particles during calcination from 600 to 1000 °C. The XRD patterns clearly showed that the mixed oxides calcined at 1000 °C had cubic structures.

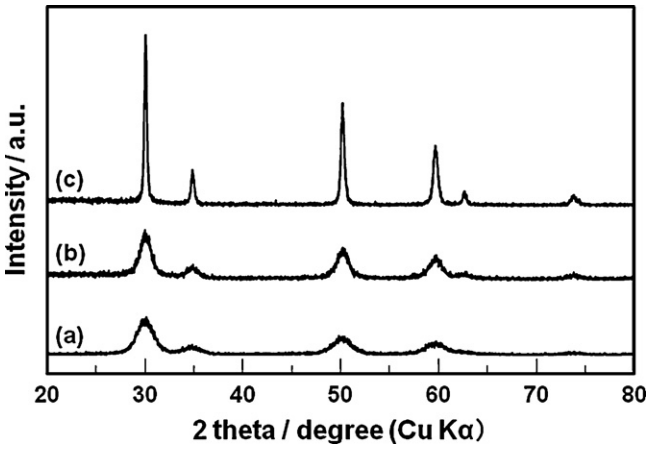


**Fig. 1.** XRD patterns of 8YSZ after glycothermal treatment (a) 8YSZ-non, (b) 8YSZ-600, and (c) 8YSZ-1000.

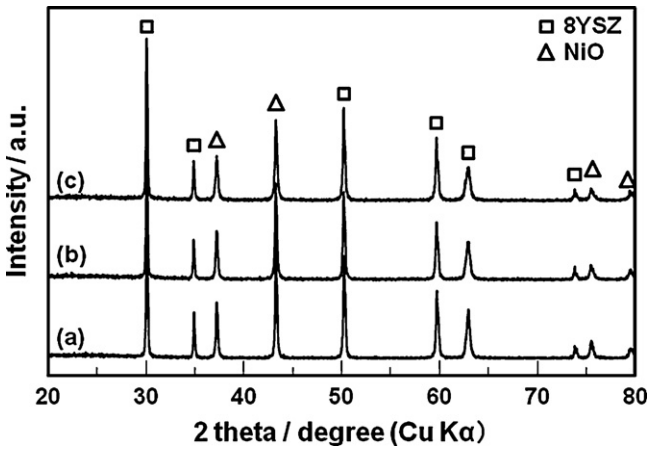


**Fig. 2.** XRD patterns of Ni/8YSZ after calcination at 1400 °C (a) Ni/8YSZ-non-1400, (b) Ni/8YSZ-600-1400, and (c) Ni/8YSZ-1000-1400.

Fig. 2 shows XRD patterns for Ni/8YSZ-non-1400, Ni/8YSZ-600-1400 and Ni/8YSZ-1000-1400. There was no structural difference among the anodes. Table 1 shows the crystallite sizes of NiO and 8YSZ in Ni/8YSZ calculated from Sherrer's equations. The crystallite size of NiO ranged from 45 to 48 nm, and that of 8YSZ ranged from 29 to 32 nm. The crystallite sizes of NiO for anodes were almost same regardless of crystallite sizes of 8YSZ.

### 3.2. Carbon deposition on anode catalysts

The rate of carbon deposition for steam reforming of methane was measured on a thermobalance. Many researchers have agreed that the rate of steam reforming of methane on $Ni/Al_2O_3$ catalysts is proportional to partial pressure of methane and that the rate is independent of partial pressure of water [19–21].

$CH_4 \rightarrow C + 2H_2$ Rate of, $CH_4$ decomposition :$R_1$

The above $CH_4$ decomposition is the rate-determining step.

$C + H_2O \rightarrow CO + H_2$ Rate of C removal :$R_2$

The rate of coke deposition depends on the combination of the above reactions.

$R(\text{coke formation}) = R_1 - R_2.$

For practical generation in an IR-SOFC, the $H_2O/CH_4$ (steam/carbon, S/C) ratio is usually over 2 under a pressurized condition. These values are far from a thermodynamically carbon deposition condition. However, deactivation by coke deposition is a serious problem for long-time operation even under this TCDC. Therefore, it is important to evaluate the rate of carbon deposition under a TCDC, which is similar to a practical generation condition for an IR-SOFC.

We calculated thermodynamics of carbon deposition. The relation between $H_2O/CH_4$ and $CH_4$ conversion is shown in Fig. 3. When $CH_4$ is decomposed at a high rate with a low $H_2O/CH_4$ ratio, it is thermodynamically impossible to remove all of the carbon deposited. The rate of $CH_4$ decomposition was fixed ($CH_4$ conversion: 35%) by changing the catalyst weight. This means that the rate of $CH_4$ decomposition, $R_1$, was fixed. Calculation showed

**Table 1**
Crystallite size of NiO and 8YSZ in Ni/8YSZ after calcination at 1400 °C.

| Anode | Crystallite size of NiO/nm | Crystallite size of 8YSZ/nm |
|---|---|---|
| Ni/8YSZ-non-1400 | 48.1 | 29.2 |
| Ni/8YSZ-600-1400 | 45.4 | 31.8 |
| Ni/8YSZ-1000-1400 | 45.2 | 29.2 |

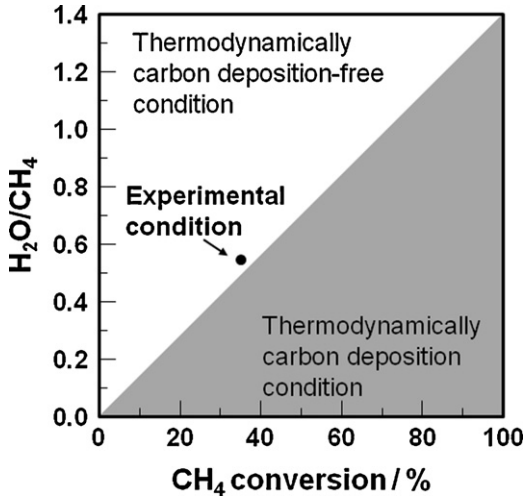


**Fig. 3.** Relation between $H_2O/CH_4$ and $CH_4$ conversion obtained by thermodynamic calculation.

that coke is not thermodynamically formed when $H_2O$ concentration is more than 9.4%, ($H_2O/CH_4 > 0.49$). When $H_2O$ was 10.6%, ($H_2O/CH_4 > 0.55$), the rate of coke formation was kinetically controlled, not thermodynamically.

Fig. 4 shows carbon deposition rates of various Ni cermet anode catalysts. Ni/8YSZ-1000-1400 showed the highest rate of carbon deposition. Since commercial 8YSZ is close to 8YSZ-1000, Ni/8YSZ-1000-1400 is the closest to a conventional Ni cermet anode catalyst. The carbon deposition rate decreased with a decrease in crystallite size of 8YSZ. This difference in carbon deposition rate among Ni cermet anode catalysts might be caused by the difference in interaction between Ni and YSZ. At the same time, crystallite size may be another reason, because the reaction for coke formation needs more active sites. In our case, Ni/8YSZ anode catalysts were prepared from 8YSZ with different crystallite size. However, crystallite size of all catalysts used was the same after calcination at 1400 °C as shown in Table 1 and the amount of active site is almost same among catalysts. Therefore, crystallite site of Ni/8YSZ did not affect the difference of carbon deposition reaction. Also, the crystallite size of Ni in Ni/8YSZ was enough to occur carbon deposition.

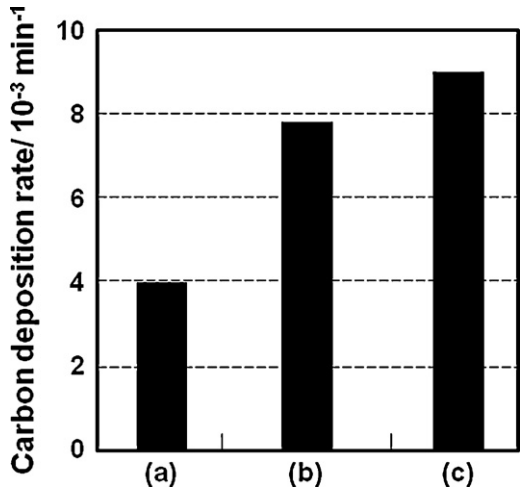


**Fig. 4.** Effect of carbon deposition rate for the first 10 min on steam reforming of methane on various Ni-anodes under a thermodynamically coke deposition-free condition. Gas composition: 19.3% $CH_4$, 10.6% $H_2O$, balance $N_2$; Total flow rate: 60 STP ml $min^{-1}$; Reaction temperature: 1000 °C. Conversions of all samples were fixed to about 35% (a) Ni/8YSZ-non-1400, (b) Ni/8YSZ-600-1400, and (c) Ni/8YSZ-1000-1400.

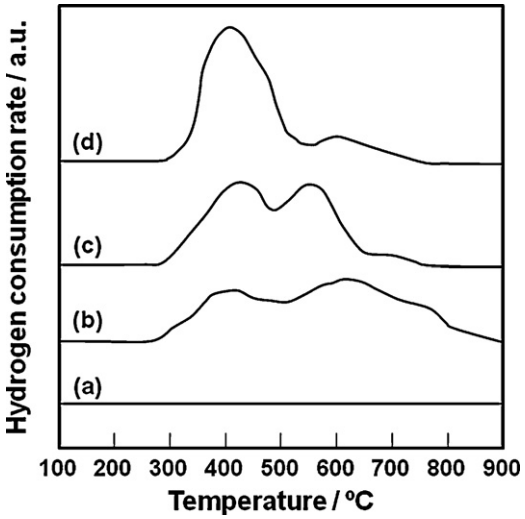


**Fig. 5.** TPR profiles of Ni cermet anode catalysts (a) 8YSZ calcined at 1400 °C, (b) Ni/8YSZ-non-1400, (c) Ni/8YSZ-600-1400, and (d) Ni/8YSZ-1000-1400.

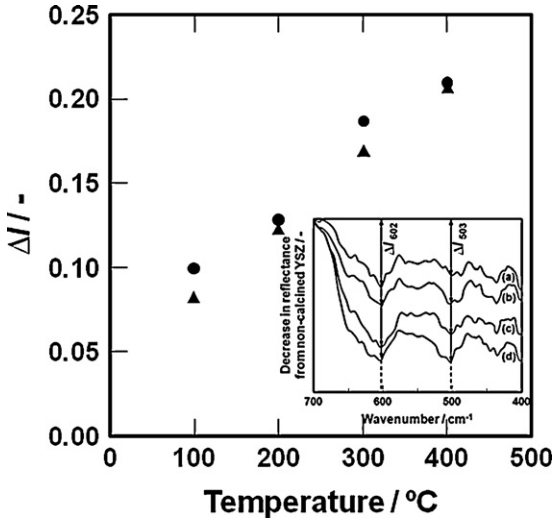


**Fig. 6.** Decrease in reflectance at 503 (●) and 602 $cm^{-1}$ (▲) at various temperatures (inset) in situ IR spectra of YSZ calcined at (a) 100 °C, (b) 200 °C, (c) 300 °C and (d) 400 °C. All spectra were referenced to non-calcined YSZ.

### 3.3. Interaction between Ni and YSZ (TPR)

Temperature-programmed reduction (TPR) profiles of Ni/8YSZ under flowing 5% $H_2$–Ar are shown in Fig. 5. Reduction of nickel oxide in the cermet was initiated at ca. 300–400 °C for each sample, and two reduction peaks were observed at low temperature (ca. 400–500 °C) and high temperature (>550 °C). The former peak can be attributed to reduction of NiO free from influence of the support, whereas the latter one indicates strong interaction between NiO and the support [3,22,23]. For Ni/8YSZ-non-1400, only a small amount of Ni was isolated from 8YSZ because the peak at lower temperature was small. The interaction between Ni and 8YSZ-non was the strongest because there were some reduction peaks of NiO at high temperature. For Ni/8YSZ-600-1400, there were two peaks at low temperature and intermediate temperature. This means that the Ni isolated from 8YSZ and Ni having interaction with 8YSZ coexist in the cermet. Ni/8YSZ-1000-1400 showed a main peak at low temperature, indicating weak interaction between Ni and 8YSZ-1000. Therefore, the order of interaction is as follows.

Ni/8YSZ-non-1400 > Ni/8YSZ-600-1400 > Ni/8YSZ-1000-1400

This order corresponds to the order of carbon deposition rate. The interaction between Ni and 8YSZ increased with a decrease in carbon deposition rate. Therefore, it was indicated that the interaction between Ni and the support is closely related to carbon deposition rate.

### 3.4. Surface analysis (DRIFTS)

The interaction between Ni and 8YSZ prepared by the glycothermal method was changed by changing the calcination temperature before impregnating Ni. Therefore, the surface properties of 8YSZ before and after calcination were analyzed. The support prepared by the glycothermal method consists of superfine particles, and there are many surface hydroxide groups on 8YSZ. The surface hydroxide groups were analyzed by in situ FT-IR. Inset in Fig. 6 shows the IR spectra of 8YSZ calcined at various temperatures, which were referenced to non-calcined YSZ. Thus peaks to a downward direction show decrease in reflectance ($\Delta I$). Peaks attributed to surface hydroxide groups were observed at 503 and 602 $cm^{-1}$ [24]. Therefore, increase in $\Delta I$ at 503 and 602 $cm^{-1}$ means the decrease in the amount of hydroxide groups. Fig. 6 shows the relation between $\Delta I$ and calcination temperature for 8YSZ. The amount of the surface hydroxide group decreased with increase in calcination temperature. A surface hydroxide group causes formation of solid solution partially. Then interaction between the supported metal and support material becomes strong. As a result, the interaction between Ni and 8YSZ decreased with increase in calcination temperature before impregnating Ni because the amount of the surface hydroxide group was decreased by calcination.

### 3.5. Electrochemical performance test

The current–voltage characteristics for SOFCs with Ni cermet anode catalysts on 8YSZ were examined in an $H_2$ stream as a fuel gas. The results are shown in Fig. 7. The open circuit voltage was around 1.09 V regardless of calcination temperature. The Ni cermet anode catalysts functioned as anode catalysts. When Ni/8YSZ-non-1400 was used as the anode catalyst, maximum power density was 200 mW $cm^{-2}$ at 500 mA $cm^{-2}$. However, Ni/8YSZ-600-1400 and

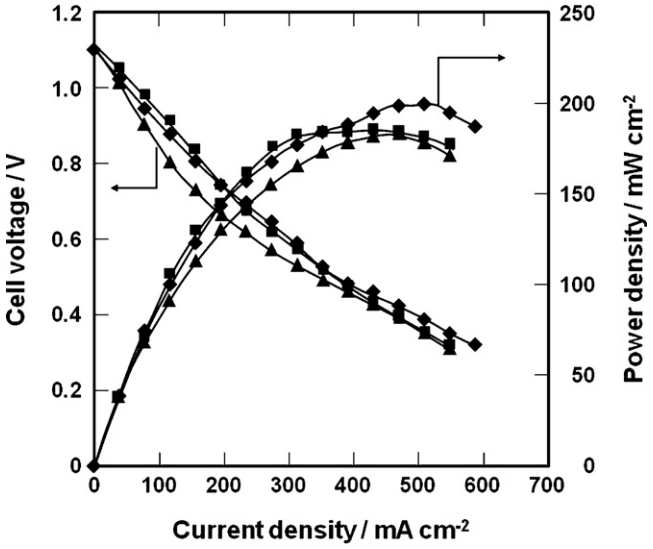


**Fig. 7.** Performances of cells with various Ni anodes for $H_2$ oxidation. (♦) Ni/8YSZ-non-1400, (■) Ni/8YSZ-600-1400, (▲) Ni/8YSZ-1000-1400. Anode gas: $H_2$ (3% $H_2O$), flow rate: 100 STP ml $min^{-1}$, Cathode gas: $O_2$; flow rate: 100 STP ml $min^{-1}$, reaction temperature: 1000 °C.

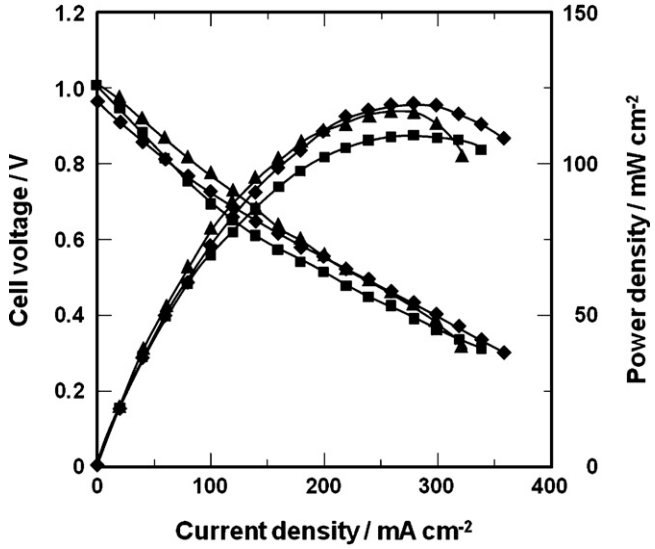


**Fig. 8.** Performances of cells with various Ni anodes for IR-SOFC in a $CH_4$–$H_2O$ stream. (♦) Ni/8YSZ-non-1400, (■) Ni/8YSZ-600-1400, (▲) Ni/8YSZ-1000-1400. Anode gas: 10% $CH_4$, 20% $H_2O$, 70% $N_2$ (balance); flow rate: 150 STP ml $min^{-1}$, cathode gas: $O_2$, flow rate: 150 STP ml $min^{-1}$; reaction temperature: 1000 °C.

Ni/8YSZ-1000-1400 showed almost the same performance as that of Ni/8YSZ-non-1400. Crystallite sizes of 8YSZ before impregnating Ni did not affect electrochemical performance for $H_2$ oxidation.

In a $CH_4$–$H_2O$ stream as a fuel gas, the current–voltage characteristics for the IR-SOFC with Ni cermet anode catalysts on 8YSZ were examined. The results are shown in Fig. 8. The open circuit voltage of the cell with Ni cermet was around 1.0 V regardless of calcination temperature. Also, all anodes showed almost the same electrochemical performance for $CH_4$. There were no effects of calcination of 8YSZ before impregnating Ni on electrochemical performance for $CH_4$ oxidation.

### 3.6. Electrochemical impedance analysis

AC impedance analysis was carried out for cells with Ni cermets as shown in Fig. 9. Ohmic resistance was determined by the high-frequency intercept with the abscissa, and non-ohmic resistance was determined from the distance between low- and high-frequency intercepts with the abscissa [14,25–27]. Anode interface resistance, $R_A$, corresponds to non-ohmic resistance because a common electrolyte, YSZ, is used. The ohmic resistance and $R_A$ of all cells was 1.3–1.5 Ω and about 4.8 Ω, respectively. All anodes showed almost the same resistance regardless of calcination temperature. These results are in agreement with results for electrochemical performance.

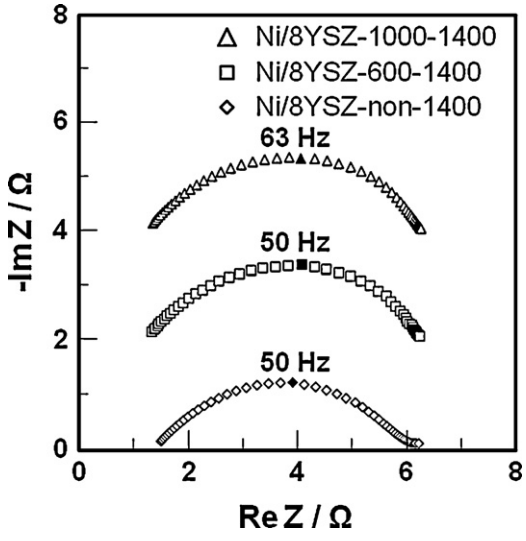


**Fig. 9.** AC impedance of cells with various Ni anodes for SOFC at OCV for $H_2$ oxidation at 1000 °C.

Although Ni/8YSZ-1000-1400, Ni/8YSZ-600-1400 and Ni/8YSZ-non-1400 showed almost the same electrochemical performance, the effect of suppression of carbon deposition was clearly observed for Ni/8YSZ-non-1400 as shown in Fig. 4. Ni/8YSZ-non-1400 showed strong interaction between Ni and 8YSZ. This strong interaction was caused by the presence of surface hydroxide groups. 8YSZ prepared by the glycothermal method has many surface hydroxide groups. The strong interaction between Ni and 8YSZ suppresses agglomeration of Ni particles. Thus, carbon deposition was inhibited. Matsui et al. [3] reported earlier that the interaction between Ni and ScSZ strongly influences the carbon deposition rate. In this literature, Ni–ScSZ treated at 1400 °C showed low carbon resistivity. The main reason for this result was Ni agglomeration. Another reason was strong interaction between NiO and ScSZ because this interaction indicated partial solid solution between NiO and ScSZ, which caused the decrease in ionic conductivity of ScSZ. These results conflicts with our results. In our cases, there is a possibility that solid solution has occurred partially as described in Section 3.4. However, since all anodes showed rather similar electrochemical activity, we thought that the strong interaction between Ni and YSZ did not affect the ionic conductivity as shown in Figs. 7 and 8, and improved carbon resistivity. Also, there is a possibility that the support material reduces carbon deposition on the catalyst. We have reported that deposited carbon can be reduced by reaction with $O^{2-}$, which is sourced from $CeO_2$ in the anode layer [27]. Fumoto et al. reported that $ZrO_2$ exhibits activity to produce active oxygen species from $H_2O$ [28]. Defects of oxygen in $CeO_2$ can be supplied by active oxygen species. For Ni/8YSZ-1000-1400, there is a large amount of Ni isolated from 8YSZ. Therefore, it is difficult to remove carbon deposited on the Ni catalyst, because the lattice oxygen cannot react with carbon. On the other hand, Ni/8YSZ-non-1400 having Ni that strongly interacted with 8YSZ inhibited carbon deposition. Carbon deposited near Ni and 8YSZ can react with lattice oxygen in 8YSZ. Therefore, the Ni/8YSZ-non-1400 anode is a candidate for a long-time operation IR-SOFC anode catalyst. When this material is used as an SOFC anode catalyst for steam reforming of methane, it is possible to reduce the amount of water in the reactor. Reduction of water theoretically contributes to an increase in total efficiency of the SOFC [8,29]. Therefore, a cell with a carbon deposition-resistance anode is expected to exhibit high performance for electrochemical oxidation using $CH_4$ as the fuel gas.

## 4. Conclusions

We prepared Ni cermet anodes from nanoparticle 8YSZ calcined at various temperatures. The electrochemical performances of the anodes were almost same regardless of calcination temperature. However, a Ni cermet anode prepared from 8YSZ without calcination inhibited carbon deposition during steam reforming of methane. This high carbon deposition resistivity was caused by strong interaction between Ni and YSZ, which was enhanced by the presence of surface hydroxide groups.

## References

[1] G.J. Saunders, J. Preece, K. Kendal, J. Power Sources 131 (2004) 23–26.
[2] S. McIntosh, R.J. Gorte, Chem. Rev. 104 (2004) 4845–4865.

[3] T. Matsui, T. Iida, R. Kikuchi, M. Kawano, T. Inagaki, K. Eguchi, J. Electrochem. Soc. 155 (2008) B1136–B1140.
[4] F.N. Cayan, M. Zhi, S.R. Pakalapati, I. Celik, N. Wu, R. Gemmen, J. Power Sources 185 (2008) 595–602.
[5] R.S. Gemmen, J. Trembly, J. Power Sources 161 (2006) 1084–1095.
[6] J.V. Herle, Y. Membrez, O. Bucheli, J. Power Sources 127 (2004) 300–312.
[7] H. Saito, S. Hasegawa, M. Ihara, J. Electrochem. Soc. 155 (2008) B443–B447.
[8] T. Takeguchi, Y. Kani, T. Yano, R. Kikuchi, K. Eguchi, K. Tsujimoto, Y. Uchida, A. Ueno, K. Omoshiki, M. Amezawa, J. Power Sources 112 (2002) 588–595.
[9] S. Park, J.M. Vohs, R.J. Gorte, Nature 404 (2000) 265–267.
[10] M.D. Gross, J.M. Vohs, R.J. Gorte, J. Mater. Chem. 17 (2007) 3071–3077.
[11] A. Atkinson, S. Barnett, R.J. Gorte, J.T.S. Irvine, A. McEvoy, M. Mogensen, S.C. Singhal, J. Vohs, Nat. Mater. 3 (2004) 17–27.
[12] S. Tao, J.T.S. Irvine, J. Electrochem. Soc. 151 (2004) A252–A259.
[13] J.C. Ruiz-Morales, J. Canales-Va'zquez, C. Savaniu, D. Marrero-Lo'pez, W. Zhou, J.T.S. Irvine, Nature 439 (2006) 568–571.
[14] S. Lee, G. Kim, J.M. Vohs, R.J. Gorte, J. Electrochem. Soc. 155 (2008) B1179–B1183.
[15] M. Inoue, H. Kominami, T. Inui, Appl. Catal. A 97 (1993) L25–L30.
[16] T. Matsui, R. Kishida, J.-Y. Kim, H. Muroyama, K. Eguchi, J. Electrochem. Soc. 157 (2010) B776–B781.
[17] B. Iwanschitz, J. Sfeir, A. Mai, M. Schützeb, J. Electrochem. Soc. 157 (2010) B269–B278.
[18] D. Sarantaridis, R.J. Chater, A. Atkinson, J. Electrochem. Soc. 155 (2008) B467–B472.
[19] P. Münster, H.J. Grabke, J. Catal. 72 (1981) 279–287.
[20] I.M. Bodrov, L.O. Apel'baum, M.I. Temkin, Kinet. Katal. 9 (1968) 1065–1071.
[21] W.W. Akres, D.P. Camp, AIChE J. 1 (1955) 471–475.
[22] H. Mori, C. Wen, J. Otomo, K. Eguchi, H. Takahashi, Appl. Catal. A 245 (2003) 79–85.
[23] Y. Zhang, B. Liu, B. Tu, Y. Dong, M. Cheng, Solid State Ionics 176 (2005) 2193–2199.
[24] R. Reshmi, G. Sangay, S. Sugunan, Catal. Commun. 8 (2007) 393–399.
[25] T. Horita, K. Yamaji, N. Sakai, H. Yokokawa, A. Weber, E. Ivers-Tiffée, Electrochim. Acta 46 (2001) 1837–1845.
[26] M.D. Gross, K.M. Carver, M.A. Deighan, A. Schenkel, B.M. Smith, A.Z. Yee, J. Electrochem. Soc. 156 (2009) B540–B545.
[27] H. Takahashi, T. Takeguchi, N. Yamamoto, W. Ueda, Solid State Ionics 185 (2011) 52–57.
[28] E. Fumoto, T. Tago, T. Tsuji, T. Masuda, Energy Fuels 18 (2004) 1770–1774.
[29] K. Eguchi, H. kojo, T. Takeguchi, R. Kikuchi, K. Sasaki, Solid State Ionics 152–153 (2002) 411–416.